

Polymer–gas interactions at high pressure: the use of ultrasonic probes

B. J. Briscoe and S. Zakaria

Chemical Engineering Department, Imperial College, Prince Consort Road, London SW7, UK

(Received 29 March 1989; revised 19 June 1989; accepted 22 August 1989)

This paper describes the use of ultrasonic transducers to estimate the physical and mechanical changes produced in organic polymers when they are subjected to high pressure gas media. Two experimental methods, involving the use of commercial ultrasonic transducers, are outlined to exemplify the potential of the techniques. One method uses a transducer as a simple displacement probe where the linear strain in the sample is sensed by measuring an acoustic distance in a liquid chamber attached to the sample. A second method measures an acoustic length in the sample itself. Both methods require appropriate calibration. The second technique also provides data on the physical state of the sample, in particular the acoustic modulus and the formation of internal fissures or bubbles which may be generated in fluctuating gas pressure fields.

(Keywords: ultrasonic transducers; organic polymers; polymer–gas interaction)

INTRODUCTION

Organic polymers absorb appreciable quantities of gas when they are exposed to a high pressure gas. The mass sorbed, or indeed desorbed, following a change in ambient gas pressure is time dependent but usually an equilibrium gas solubility is achieved after a suitably long period of time. This kinetic behaviour is, of course, governed by the permeability of the gas in the polymer under the prevailing ambient conditions. Hence the gas saturation times are a function of the particular combination of the gas, the polymer, the temperature and the ambient pressure. Similarly, the equilibrium mass solubility is a function of the same variables. At the 'equilibrium' condition the mass sorbed by many polymers is in proportion to the ambient gas density. In addition the prevailing gas pressure appears to induce a triaxial stress on the polymer. In some cases, notably PTFE, the polymer contracts¹ although the elastomer considered here dilates.

Thus, when the polymer is equilibrated in a high pressure gas environment it contains a uniform excess gas concentration² and a relative compressive triaxial stress compared with its equilibrium state at a lower ambient pressure. As a result, when the ambient pressure is reduced a negative (tensile) triaxial stress is produced³ and also an internal stress gradient is created associated with the developing gas concentration profiles within the polymer⁴. The existence of these stress fields has not been confirmed directly although the present study provides data consistent with this model. It is generally known that when the environment surrounding a polymer is decompressed rapidly it may rupture the polymer in a manner consistent with the presence of these types of stress fields. The phenomenon is termed 'explosive decompression failure' and a few references to the process may be found in the scientific and technical literature^{5–7}. Certain studies have also addressed the effect of a negative triaxial stress on polymers when the stress is produced by the action of confined tensile forces^{8,9}.

A number of central questions emerge upon a detailed examination of the origin of this phenomenon. Important

factors are the time (or the ambient pressure) during the decompression when the polymer ruptures internally and the volume of the sample at this occurrence. In addition, it is necessary to estimate the modulus of the polymer under the high pressure ambient conditions in order to predict the failure stress required to induce cavitation voids or cracks in the polymer. A first order solution, for example, predicts cavitation at a negative triaxial stress of 5/6 times the Young's modulus⁸ and corresponding volumetric dilation strain of *c.* 3% (ref. 14).

In this paper, we mainly describe two experimental configurations which use the ultrasonic pulse echo technique¹⁰ to enable the measurement of these characteristics. The polymeric samples to be described were studied in the form of relatively short, parallel-faced cylinders. The two techniques have been evaluated using a silicone elastomer, a nitrile rubber and a PTFE in a pressure range of *c.* 0.1 to 27 MPa using nitrogen gas at ambient temperature. The first arrangement (later described as mode-1) is applicable to soft rubbery materials that can be readily and reasonably pre-strained. In this method the ultrasonic transducer was located in direct contact with the plane face of the specimen. The change in the transit time between successive reflections from its back face is measured as a function of ambient gas pressure. This variation is a function of the changes in the modulus, the density and the dimensions of the specimen. The attenuation in the transmitted signal during transient decompression of the ambient gas provides information about the crack nucleation and propagation or bubble nucleation and inflation which may be produced within the polymer. In the second method (mode-2) the ultrasonic transducer is not in direct contact with the specimen. The transducer is partially immersed in a liquid contained in a small container which is placed on one of the plane surfaces of the specimen. This method can only monitor the dimensional changes in polymers that accompany gas pressurization and decompression. The sensitivity and accuracy of these two methods depends upon the precision of the measurement of the transit time and hence upon the frequency of transmitted signal and

the data sampling frequency. Specifically, we will show how this ultrasonic technique can provide data on the variation of the linear strain and other physical property changes in an elastomer as a function of pressure under quasi-equilibrium conditions and also when the pressure is rapidly reduced. In conjunction with results obtained from a special gravimetric technique, the data from the ultrasonic method also provides an accurate estimate of the acoustic modulus of non-dispersive polymers in high pressure gas media. In addition, we will demonstrate how one experimental arrangement also senses the later stages of extended explosive rupture in certain polymers. In combination the various techniques provide unique and relevant information about the nature of the polymer-gas interactions at high ambient gas pressure.

MATERIALS AND EXPERIMENTAL METHODS

Materials

The polymers used in this study were a silicone elastomer (Dow Corning Sylgard 184) density 1.023 g cm^{-3} , a carbon filled nitrile rubber (BP Chemicals) density 1.22 g cm^{-3} and a PTFE (ICI) density 2.089 g cm^{-3} . The nitrogen gas used as the pressurizing media was 'white spot', oxygen free.

Apparatus

Hydrostatic compressibility. The bulk compressibility of the polymeric samples was investigated using a conventional mercury porosimeter (Carlo Erba, Italy). Small polymeric samples ($25 \times 8 \times 5 \text{ mm}$) were introduced into a glass dilatometer to which was attached a capillary tube. The system was evacuated to $c. 10^{-3}$ torr and charged with mercury. The hydrostatic pressure transmitting medium, which was isolated from the sample, was ethanol. The maximum pressure of $c. 100 \text{ MPa}$, on a specimen, was achieved in approximately 2 h. The volume change was sensed by following the position of the mercury-ethanol interface in the capillary. Correction was made for the compressibility of mercury. The data presented here are for the first compression of the samples.

High pneumatic pressure studies

General pressure vessel assembly. The pressure vessel assembly consisted of a compressed air driven reciprocating gas booster pump (Charles Madan, Altrincham, England) capable of producing a pressure of up to $c. 60 \text{ MPa}$ from a gas bottle at $c. 6 \text{ MPa}$. An intermediate gas receiver was used between the compressor and the pressure vessel to smooth the pressure fluctuations during pressurization. The pressure vessel employed was 610 mm long with an o.d. of 127 mm and an i.d. of 50.8 mm and was housed in a thermostat chamber; temperature $\pm 1^\circ\text{C}$. The gas pressure was released manually through a 3 mm needle valve. A more detailed description of the whole assembly has been given elsewhere¹¹.

Mass sorption. The 'equilibrium' gas mass sorption of the polymer was measured by a vibrating reed technique which has been described in detail elsewhere¹¹. The elastomer sample $28 \times 8 \times 6 \text{ mm}$ ($c. 1.4 \text{ g}$) was attached to the end of a thin metal reed such that its largest axis was orthogonal to the major axis of the reed. The reed was vibrated by the action of a solenoid and the vibration of the beam was sensed by a strain gauge attached to the reed. The experimental procedures, methods of calibra-

tion and data computation are detailed in another publication¹¹. Essentially, the method involves measuring the change in the natural vibrating frequency of the reed (typically 180 Hz) as the rest mass (polymer + sorbed gas) changes. By its nature this type of experiment also entrains an envelope of gas around the sample of approximately a constant but unknown volume; the so called entrained mass. A calibration of this contribution to the measured rest mass requires using an aluminium sample of similar size and geometry to the elastomeric sample. The data quoted in this paper and described here as 'equilibrium' data correspond to the mass sorption after at least 45 min exposure to each increment of gas pressure. We performed long term studies to establish that no detectable changes in sorbed mass were observed after this period of time for the samples of this size. The mass sensitivity of the device used in this study was $\pm 0.1 \text{ mg}$. The pressure was actually increased in incremental ramps and the samples were, for obvious reasons, not rapidly decompressed. Hence, the mass sorption quoted for the high pressures will have received an accumulated exposure of several hours at increasingly higher pressures.

Ultrasonic system

Electrical connections and data acquisition. The instrumentation involved in these techniques essentially consisted of piezoelectric transducers, a pulse generator, an amplifier, an oscilloscope and a computer controlled high speed digital data acquisition system (Figures 1 and 2). The technique has not been described elsewhere and hence its construction, operation and capabilities are given in some detail. The contact type piezoelectric ultrasonic transducers of $c. 1 \text{ MHz}$ resonant frequency were built in stainless steel casings by Rolls Royce Mateval (England). These single crystal transducers could be used as signal transmitters and receivers. Small holes of $c. 1 \text{ mm}$ diameter were drilled in their casings near the back non-active face so that the high ambient pressure

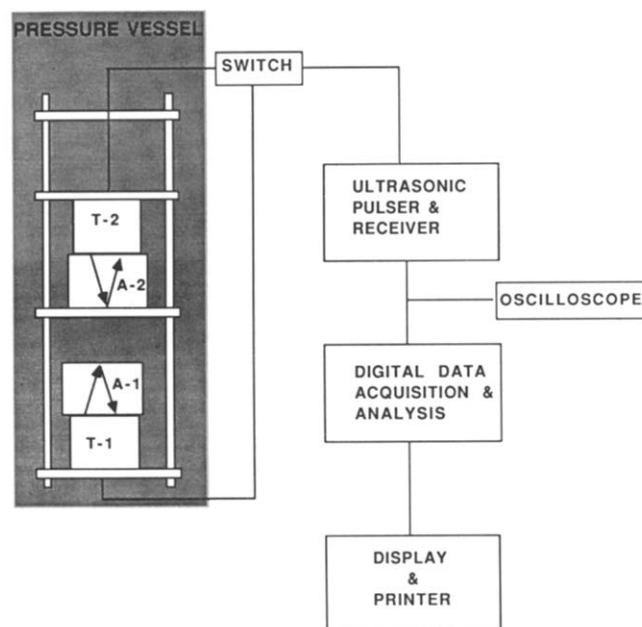


Figure 1 Mode-1 experimental arrangement and accompanied data acquisition electronics: T-1, T-2, ultrasonic transducers; A-1, A-2, polymeric specimen

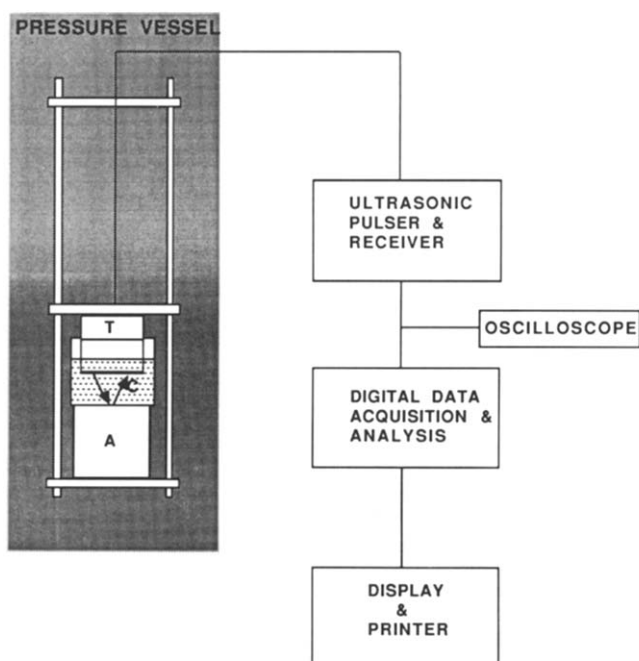


Figure 2 Mode-2 experimental arrangement and accompanied data acquisition electronics: T, ultrasonic transducer; A, polymeric specimen; C, signal transmitting liquid

was balanced inside the casing cavity. Most transducers of this type are constructed with a polymeric damping component which encapsulates the free surfaces of the piezoelectric crystal. This polymer is quite vulnerable to gas desorption induced rupture in certain environments. This is particularly so in CO_2 media for example. The ultrasonic transducer was connected to a pulser-receiver unit (Panametrics, Inc., Model 5052 PRX75). The signals were captured by a software driven digital data acquisition board (WAAG, Wave acquisition and generation, Markenrich, Inc., USA) sitting in an expansion slot of an IBM XT computer. The data sampling frequency range of the board was from 2 kHz to 20 MHz. It was triggered by the synchronizing signal from the pulser-receiver unit. The software used sets aside a block of the computer memory for the data and a maximum of 40 acquisition sets of 1400 data points each could be stored. The number of data points acquired in each set at 20 MHz sampling frequency were sufficient to record the original input pulse and its first and the second echoes from the opposite face of the specimen. The captured data arrays were transferred from the computer RAM to its hard disc and analysed subsequently.

Mode-1. Figure 1 shows a schematic diagram of the experimental arrangement. The transducers were in direct contact with the specimens with a thin layer of acoustic coupling grease between the interfaces to ensure a uniform contact. The transducers were mounted on a metallic frame and housed in the gas pressure vessel. The polymeric specimens used in the experiment were cylindrical, *c.* 25 mm diameter and *c.* 15 mm thick and care was taken to maintain the specimen faces parallel and smooth. An unconstrained specimen (A-1, Figure 1) was placed on one transducer. The second transducer was directly loaded on to the other specimen by one of the circular discs in the brass frame and this specimen (A-2, Figure 1) was strained to *c.* 10%. The strained specimen was a reference in this experiment because it was assumed

that any change in the transit time under high pressure was not due to dimensional changes in the sample and the brass frame. This assumption introduces an error in the magnitude of the estimated linear strain of *c.* 1.0%. The bulk modulus of the brass is a factor of *c.* 100 greater than that of the elastomer. No correction is made for this effect as it is within the experimental uncertainty of the data. This whole assembly, consisting of the ultrasonic transducers and the specimens, was attached to the pressure vessel cap.

Mode-2. The experimental arrangement was similar to that used in mode-1 (Figure 2). Only one transducer (T) was used in this mode. It was held, partially dipped in distilled water (C), inside a small container that was placed on the upper plane surface of the specimen (A) to be tested. Distilled water was used because its acoustic properties are well known and have also been studied extensively under high pressures^{12,13}. The water provides a uniform path for the transmission of ultrasonic signals because the problem of air entrapment associated with more viscous fluids does not occur. The acoustic length of water in the container was adjusted relative to the anticipated increase in the specimen length due to the release of gas pressure in the experiment. Signals from the transducer travelled through the water and were reflected back from the base of the beaker. This arrangement acted as a simple but effective displacement transducer and was suitable for highly attenuating specimens where the ultrasonic signals were difficult to transmit and detect. Dimensional variations in specimens over the whole pressurization cycle could also be measured. The formation of cracks in the specimen on gas decompression did not affect the ability of this method to detect these changes. The direct contact method could not provide this information after the cracks had nucleated in the elastomeric specimen because they scatter and severely attenuate the transmitted ultrasonic signal. The variation of sound velocity in the distilled water under gas pressure and the transient variations during gas decompression were evaluated separately as a necessary calibration.

DATA ANALYSIS

The pulse response characteristics of the current ultrasonic transducers were not found to vary within our levels of detection when excited in the high pneumatic pressure environment. Hence, no transducer calibration factors were used while performing the data analysis. A typical data set consists of the large amplitude pulse sent to the ultrasonic transducer by the pulse generator and the corresponding first and second reflection signals received by the transducer from the opposite flat boundary of the medium through which the signal travelled. The sections of the data array with two consecutive echoes were selected. Correction was made for phase shift (mode-1) to obtain accurate measurements. Such sections were numerically autocorrelated and the time lag was measured. The lag was twice the transit time of the signal passing through the travelling medium.

Mode-1

The initial thickness of the specimen was known and measurement of the transit time at the start of the

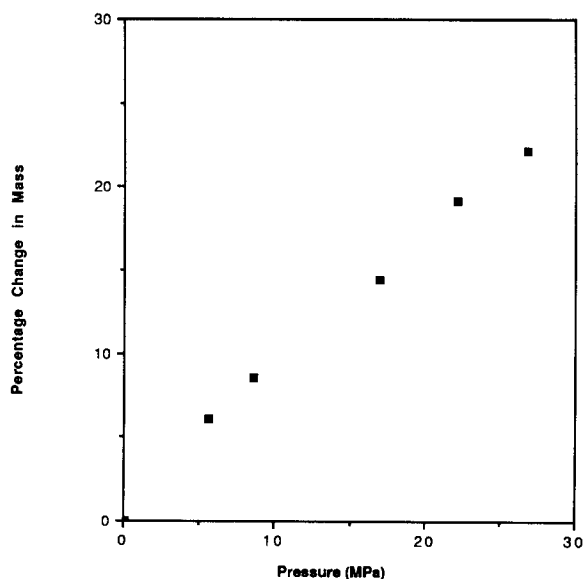


Figure 3 Percentage change in mass of silicone elastomer as a function of nitrogen gas pressure, 20°C, equilibrium time 45 min at each pneumatic pressure increment

experiment gave the velocity of sound in the material. The specimens were pressurized in steps of about 3.5–4.5 MPa using nitrogen gas. An ultrasonic signal was transmitted and the transit time was measured at that pressure. The change in the transit time was attributed to be a consequence of a combined effect of the changes in the specimen modulus, density and dimension. For the pre-strained specimen this change was assumed to result entirely from the changes in the specimen modulus and density. We, of course, assume here that the modest pre-strain, which is still within the linear stress-strain response for the elastomer, does not produce a modulus-gas pressure characteristic which is significantly different to that of the unstrained sample. The changes in the modulus will, we believe, arise from gas sorption in the specimen and the relative compression of the same by the pneumatic stress. Confinement of a test piece in a way that restricts its volumetric changes under pneumatic stress will influence the extent of gas mass absorption and thus the modulus. However, a linearly strained sample, whose height to diameter ratio is of the order of 0.6 and whose interfaces with the plates (transducer face and confinement plate) are not bonded and are able to expand diametrically, will suffer no significant additional effective hydrostatic stress on a modest pre-strain of *c.* 10%. Hence the modulus will be unaffected, whatever the ambient conditions, when compared with an unconstrained sample. This is confirmed by the fact that the change in signal velocity with pressure for different silicone elastomer test pieces, strained to various extent, remained constant (see *Figure 6*).

The specimen acoustic modulus values were computed from

$$E = V^2 \rho$$

where V is the velocity of sound, E is the modulus and ρ is the density of the material.

Significant gas uptake by some polymers at higher pneumatic pressures leads to a marked increase in their density, dimensional changes apart. The increase in density of the silicone elastomer has been determined at various pressures using the data from the vibrating reed

mass sorption sensor combined with the associated linear strain measurements obtained by the means described. Equilibrium mass uptake values at a variety of nitrogen gas pressures are given in *Figure 3*. The specimen mass and the corresponding volume value at different pressures gave its density at these conditions. The moduli of the silicone elastomer, at various pressures, were then computed using the above relationship.

The formation and development of internal cracks in the specimen during ambient pressure release have also been monitored using this experimental arrangement. The ultrasonic data were collected every 5 s while the pneumatic pressure was being reduced. Subsequently, FFT (Fast Fourier Transform) of the two consecutive back wall echoes in each set were performed. The amplitudes of the two frequency spectra were compared to determine the attenuation of the signal.

Mode-2

In this method the transit time of the ultrasonic signal was affected at high pneumatic pressure and depressurization by the change in the velocity of sound in the distilled water and the dimensional change of the specimen. The variations of sound velocity in the water have been calculated at the equilibrium conditions and during the transient conditions generated while decompressing the gas (*Figures 4* and *5*). The decompression data correspond to nonisothermal and adiabatic conditions. The gas pressure was reduced from *c.* 27 MPa to atmospheric in *c.* 5 min. These data were used to calculate the dimensional changes in the elastomeric specimen. *Figure 4* also shows the increase in the velocity of sound in distilled water with the application of a triaxial pressure. It is observed that the velocity of sound in water is more sensitive to triaxial pressure than to a nominally equivalent nitrogen gas pneumatic pressure. This difference is certainly associated with the absorption of gas in water at high pneumatic pressures. A similar trend is seen with polymers (see later). Under these conditions significant amounts of the gas were absorbed in the water

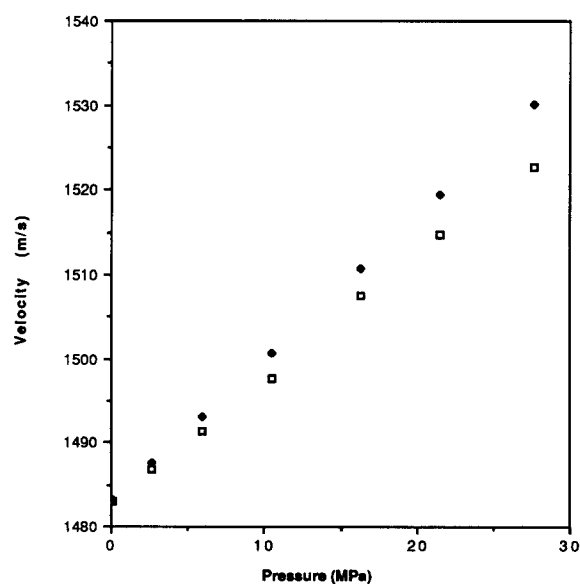


Figure 4 Change in the velocity of sound in water as a function of pressure, 20°C; □, nitrogen gas pressure, equilibrium time 45 min at each pneumatic pressure increment; ◆, triaxial pressure from reference 12

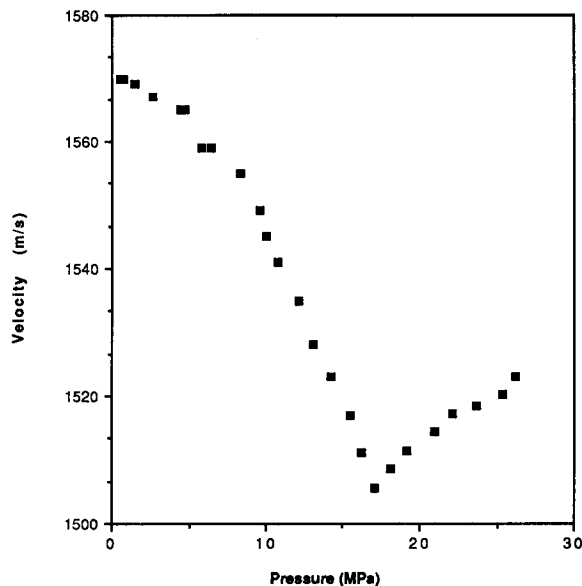


Figure 5 Velocity of sound in water during nitrogen gas depressurization (0.09 MPa s^{-1})

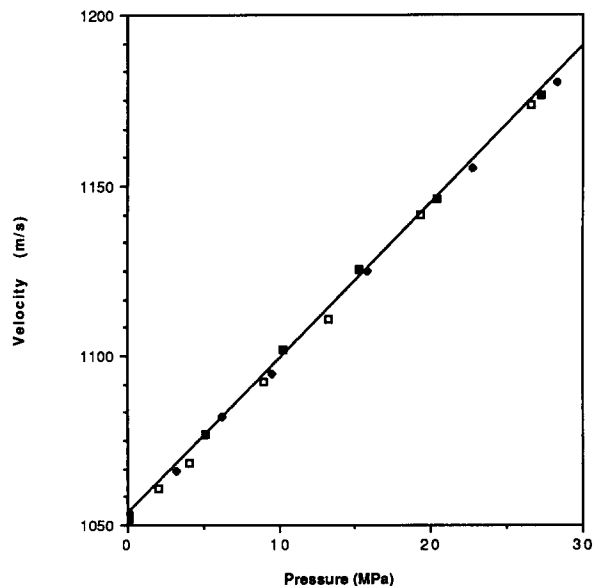


Figure 6 Change in the velocity of sound in silicone elastomer as a function of nitrogen gas pressure; \square , 7% prestrain; \blacklozenge , 10% prestrain; \blacksquare , 12% prestrain, conditions as in Figure 3.

and consequently, its density increase was higher than the case if only triaxial pressures were applied. Polymers appear to behave in a similar fashion.

EXPERIMENTAL RESULTS

The increase in the velocity of sound in the silicone elastomer at various nitrogen gas pneumatic pressures is shown in Figure 6. These velocities were measured using the mode-1 experimental method. The dimensional changes computed using both the methods (mode-1 and mode-2) for the silicone elastomer are given in Figure 7. The strain-pressure curves from both the methods correspond to an initial contraction of the specimens and subsequently a linear expansion of *c.* 1.5%. Each measurement was taken after every 45 min of isobaric conditions on an increasing pressure ramp. The system

had apparently reached mass uptake equilibrium in this period. The high pressure nitrogen gas environment induces an increase in the elastomer modulus and the density. The increment in its density at the nitrogen gas pressure of up to 27 MPa was only *c.* 17% (Figure 8). This gas pressure on the silicone elastomer resulted in a *c.* 45% increase in its computed modulus (Figure 9). During ambient pressure release the attenuation of the 1 MHz frequency component of the ultrasonic signal in the silicone elastomer is shown in Figure 10. It commences to increase with the inception of internal cracks when the decreasing pressure reaches a critical value of *c.* 18 MPa from a pressure of *c.* 27 MPa and augments rapidly with further pressure decrease until no further signals were detected by the transducer. The damage in the elastomer increases with the continuous decline in ambient pressure. The

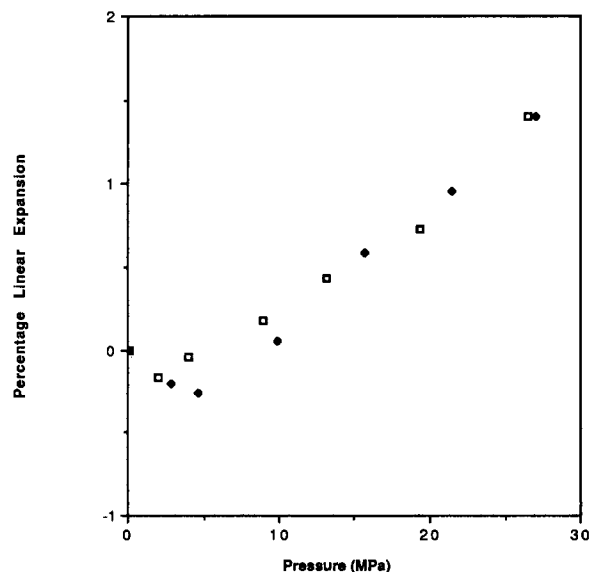


Figure 7 Percentage linear strain for silicone elastomer as a function of nitrogen gas pressure; \square , mode-1; \blacklozenge , mode-2; 20°C , equilibrium time 45 min at each pneumatic pressure increment

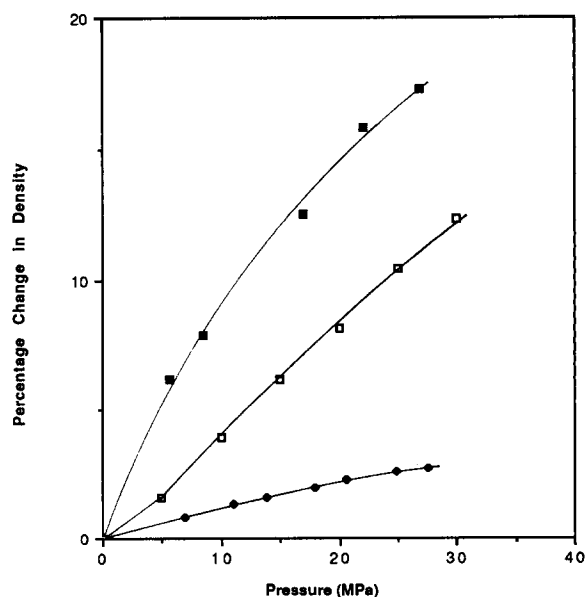


Figure 8 Computed percentage change in density, 20°C ; \blacksquare , silicone elastomer, \blacklozenge , PTFE, and \square , nitrile rubber, as a function of nitrogen gas pressure after 45 min exposure at each pressure interval

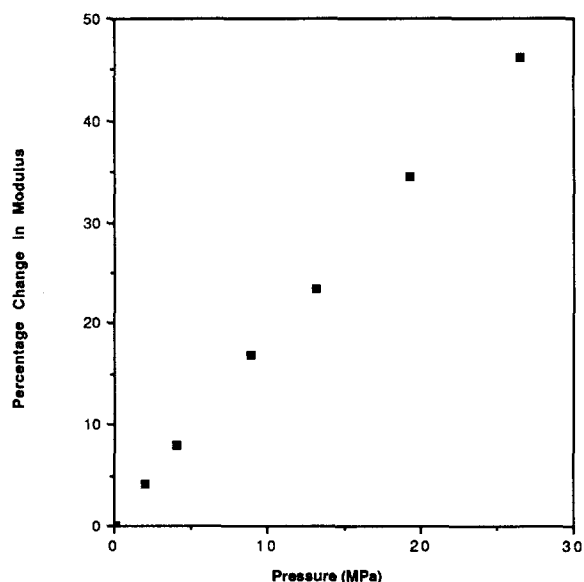


Figure 9 Percentage change in modulus for silicone elastomer as a function of nitrogen gas pressure, conditions as in Figure 8

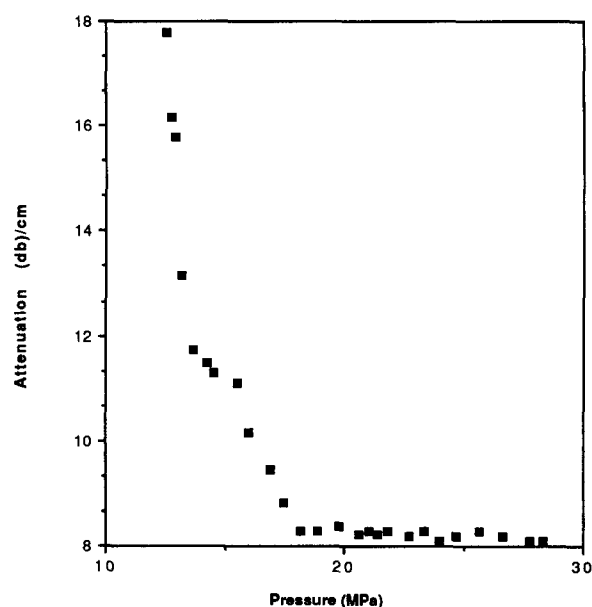


Figure 10 Attenuation of 1 MHz frequency component of the ultrasonic signal in silicone elastomer during nitrogen gas depressurization (0.09 MPa s^{-1})

the PTFE and the nitrile rubber show a linear compression of *c.* 0.4% and *c.* 0.5% respectively at *c.* 27 MPa (Figure 12). The observations for the PTFE are in agreement with the results obtained previously using a displacement transducer based upon a capacitance cell technique under similar conditions¹. However, these two polymers do not expand appreciably when the high pneumatic pressure was rapidly released.

DISCUSSION

Several generally interesting features emerge from the study of these data. First, at equilibrium, whilst the polymers described sorb significant quantities of nitrogen gas at high pneumatic pressures the associated volumetric changes are rather different. The equilibrium mass

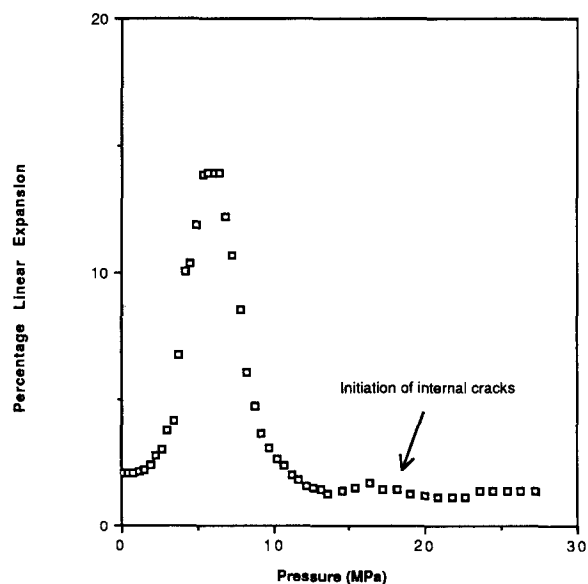


Figure 11 Percentage linear expansion for silicone elastomer during nitrogen gas depressurization, conditions as in Figure 10

internal cracks or bubbles disperse the transmitted signal and attenuate the pulse received by the transducer.

The linear expansion of the silicone elastomer in the course of the ambient pressure release was measured using the mode-2 of the experimental configuration. A significant expansion of the specimen takes place towards the end of the decompression (Figure 11). The maximum linear expansion of the specimen was *c.* 14% at *c.* 7 MPa. At this point the cracks or bubbles in the specimen would have been sufficiently developed and adequate surface area had been generated to desorb the gas at a rate equivalent to the depressurization of the ambient gas. As the pressure gradient between the polymer and surroundings and also within the polymer decreases the specimen reverts to its original size. This method (mode-2) has also been used to investigate the effects of gas pressurization on a PTFE and a nitrile rubber. Both

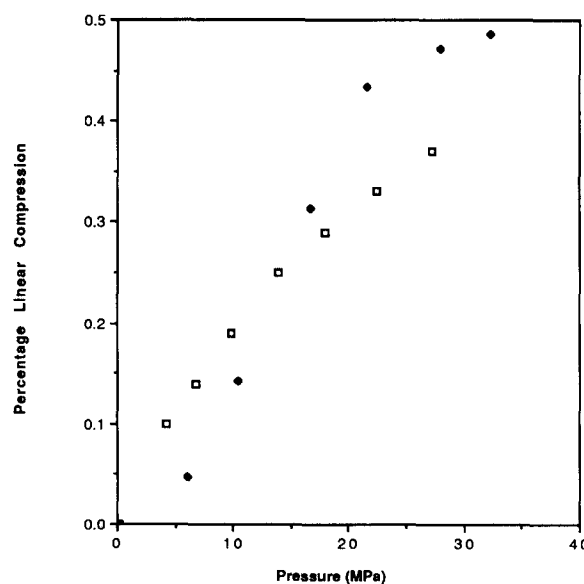


Figure 12 Percentage linear strain as a function of nitrogen gas pressure; \square , PTFE; \blacklozenge , nitrile rubber, 20°C , equilibrium time 45 min at each pneumatic pressure increment

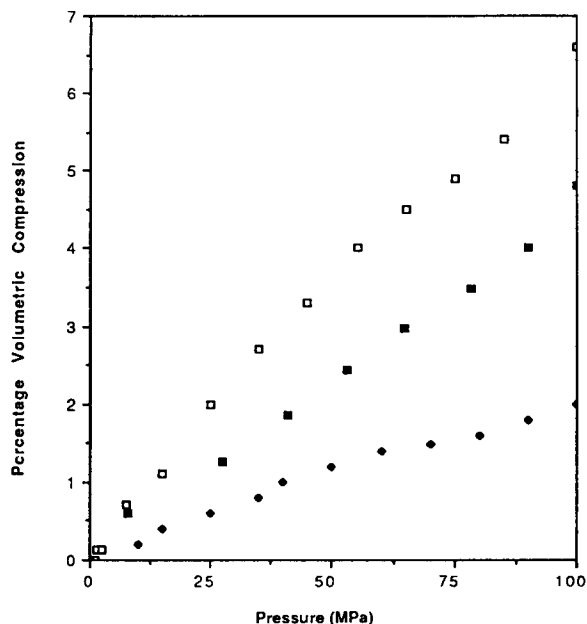


Figure 13 Percentage volumetric compression as a function of hydrostatic (mercury) pressure for degassed polymeric samples, 20°C; □, silicone elastomer; ■, nitrile rubber, ♦, PTFE

sorption to a first order is directly proportional to the ambient gas density (or pressure), for nitrogen, for all the cases. The relative nitrogen solubilities at c. 20°C are, silicone elastomer (1.0) > nitrile rubber (0.4) > PTFE (0.07). The bracketed quantities are the relative mass based solubility parameters. Considering these ratios and Figures 7 and 12, we may conclude that when sufficiently large amounts of the gas are sorbed, the system has a priority to swell in spite of an apparent triaxial compressive stress imposed by the pneumatic pressure. Thus, the PTFE and the nitrile rubber contract but the silicone elastomer initially contracts and then swells. Figure 13 shows the compressibility of these polymers under the action of triaxial stresses generated using hydrostatic stresses transmitted with mercury in the absence of gas. The trends for the pneumatic stress more or less follow the mercury triaxial stress data depending upon the extent of the gas sorption. The data for the silicone elastomer suggest that at low pressure (low gas content in the polymer) the polymer matrix is responding to a fine balance of tensile (internal) swelling stresses and compressive (external) stresses. At higher pressures the swelling stresses dominate. This behaviour is consistent with the observations made by Sekhar and Van Der Hoff¹⁵ for natural rubber when subjected to a sudden pneumatic pressure increase. The effective internal pressures created in the matrix greatly exceed the external stresses operating on the body. We may also conclude that the action of the compressive stress also reduces the extent of gas sorption by inhibiting matrix swelling. This extreme is apparently the case for the PTFE and the nitrile rubber where the gas solubility is much less at a given pressure than for the silicone elastomer.

Figure 8 shows the computed density changes for the silicone elastomer, the nitrile rubber and the PTFE as a function of the gas pressure. The mass sorption data for the nitrile rubber and the PTFE under nitrogen gas pressure were obtained from references 4 and 11, respectively. Initially the sample density increases rapidly through the combined effect of the volume reduction and

the gas mass uptake. The trend of these curves indicates that at a certain point at higher gas pressures the density will assume a constant value. Further sorption of the gas would be restricted by the pneumatic hydrostatic stress acting on the specimen and vice versa.

An examination of the sound velocity as a function of the gas pressure for the silicone elastomer (Figure 6) shows a good linear dependence upon the ambient pneumatic pressure in spite of the corresponding non-linear density-pressure relationship. The computed modulus, shown in Figure 9, as a function of pressure is considerably larger than its value in atmospheric ambient. The relative increase in the velocity of sound in the high pressure nitrogen gas environment is greater than the corresponding increase in the density of the specimen under similar conditions and therefore an overall increase in the modulus of the specimen is observed. Water responds in a similar way in high pressure nitrogen environment. The determination of the specimen modulus under the gas pressure enables the evaluation of the actual critical stress value that a polymer may withstand in a fluctuating gas pressure environment. The value of this critical stress is believed to be directly proportional to the specimen modulus^{8,9}.

In summary, the various 'equilibrium' data indicate that the polymers are apparently in a peculiar state of stress. The swelling pressure arising from sorption seeks to dilate the polymer whilst the triaxial stress compresses the polymer. The combined action of the two nominal stresses is pronounced when the pressure is reduced. During the ambient gas pressure reduction we have been able to follow only the volume changes in the silicone elastomer specimen and the generation of internal wave scattering centres such as cracks or bubbles. The crack or bubble formation processes may arise from at least two potential mechanisms: overall and localized hydrostatic tension fields followed by gas bubble or crack nucleation and growth. The suggested overall stress field will arise from the removal of the pneumatic compressive stress and this field acts uniformly over the whole sample. The so-called localized stress fields will be caused by the concentration and hence internal pneumatic pressure gradients in the sample which are produced as the gas desorbs from the specimen. The geometry and nature of the cracks produced are described in a separate publication¹⁶. These data strongly suggest that both localized hydrostatic tension and overall stress fields are produced during this type of gas desorption process. The present data do not accurately distinguish which of the two hydrostatic stress fields prevail. However, Figures 10 and 11, show that the cracks are detectable when the polymer dilates by a volumetric strain of c. 5%, which is consistent with a negative hydrostatic stress model¹⁴. However, the volumetric expansion is not instantaneous. Once the localized internal failure has occurred the cracks will inflate and gross expansion of the sample will occur as the gas desorbs into the internal voids and subsequently to the ambient. It is also possible that voids are initially present in the sample and they may inflate directly when the pressure in the bubbles exceeds the external pressure by 5/2 times the shear modulus of the elastomer⁹.

CONCLUSIONS

The use of ultrasonic pulse echo techniques has been demonstrated as a means of monitoring certain aspects of

polymer behaviour under extreme conditions of pneumatic pressure. The mode-1 technique can provide information about physical and mechanical property changes which result from pneumatic pressurization and depressurization. It also has the potential to determine the inception of fracture or bubble growth in the polymer during gas decompression. The mode-2 method, which uses the technique as a displacement cell, can only provide data on the dimensional changes associated with the pneumatic pressure cycle. The data serve to illustrate the peculiar stress fields which are created in polymers under high pneumatic pressure ambients and the consequences of rapidly reducing the ambient pressures.

ACKNOWLEDGEMENTS

The authors wish to express their thanks to Mr Steve Roach for writing the software to operate the data acquisition board used in the ultrasonic experiments and to Mr Len Moulder for general discussions on the subject.

REFERENCES

- 1 Briscoe, B. J. and Mahgerefteh, H. *J. Phys. E: Sci. Instrum.* 1984, **17**, 483
- 2 Fleming, G. K. and Koros, W. J. *Macromolecules* 1986, **19**, 2285
- 3 Gent, A. N. and Tompkins, D. A. *J. Appl. Phys.* 1969, **40**, 2520
- 4 Briscoe, B. J. and Liatsis, D. *J. Appl. Polym. Sci.*, in press
- 5 Ender, D. H. *Chemtech.* 1986, **16**, 52
- 6 Eudes, M., Langlois, M., Narcy, P., Dejeux, M. A. and Moret, D. *Nucl. Engng* 1968, **7**, 586
- 7 Wolcott, H. A. and Straznickas, S. R. Energy Sources Technology Conference and Exhibition, Dallas, Texas, February, 1985
- 8 Gent, A. N. and Lindley, P. B. *Proc. R. Soc. A* 1959, **249**, 195
- 9 Gent, A. N. and Tompkins, D. A. *J. Polym. Sci. A2* 1969, **7**, 1483
- 10 Breazeak, M. A., Cantrell, J. H. Jr and Hayman, J. S. in 'Methods of Experimental Physics', Vol. 19 (Ed. P. D. Edmonds), Academic Press, London, 1981, 67
- 11 Briscoe, B. J. and Mahgerefteh, H. *J. Phys. E: Sci. Instrum.* 1984, **17**, 1071
- 12 Wilson, W. D. *J. Acoust. Soc. Am.* 1959, **31**, 1067
- 13 Urlick, R. J. 'Principles of Under Water Sound for Engineers', McGraw-Hill, New York, 1967
- 14 Lindsey, G. H. *J. Appl. Phys.* 1967, **38**, 4843
- 15 Sekhar, N. and Van Der Hoff, B. M. E. *J. Appl. Polym. Sci.* 1971, **15**, 169
- 16 Briscoe, B. J. and Zakaria, S. *J. Mater. Sci.*, in press